Molecular Simulation
Publication details, including instructions for authors and subscription information:
http://www.tandfonline.com/loi/gmos20

Anomalous lateral diffusion in lipid bilayers observed by molecular dynamics simulations with atomistic and coarse-grained force fields

Sławomir Stachura[ab] & Gerald R. Kneller[abc]

[a] Centre de Biophysique Moléculaire, CNRS, Rue Charles Sadron, 45071, Orléans, France

[b] Synchrotron Soleil, L'Orme de Merisiers, 91192, Gif-sur-Yvette, France

[c] Université d'Orléans, Chateau de la Source-Av. du Parc Floral, 45067, Orléans, France

Published online: 24 Dec 2013.

To cite this article: Sławomir Stachura & Gerald R. Kneller (2014) Anomalous lateral diffusion in lipid bilayers observed by molecular dynamics simulations with atomistic and coarse-grained force fields, Molecular Simulation, 40:1-3, 245-250, DOI: 10.1080/08927022.2013.840902

To link to this article: http://dx.doi.org/10.1080/08927022.2013.840902

Molecular Simulation, 2014
Vol. 40, Nos. 1–3, 245–250, http://dx.doi.org/10.1080/08927022.2013.840902

Taylor & Francis
Taylor & Francis Group

Anomalous lateral diffusion in lipid bilayers observed by molecular dynamics simulations with atomistic and coarse-grained force fields

Sławomir Stachura[a,b] and Gerald R. Kneller[a,b,c]*

[a]*Centre de Biophysique Moléculaire, CNRS, Rue Charles Sadron, 45071 Orléans, France;* [b]*Synchrotron Soleil, L'Orme de Merisiers, 91192 Gif-sur-Yvette, France;* [c]*Université d'Orléans, Chateau de la Source-Av. du Parc Floral, 45067 Orléans, France*

(*Received 30 June 2013; final version received 28 August 2013*)

In this article we study the lateral molecular diffusion in homogeneous lipid 1-palmitoyl-2-oleoyl-sn-glycero-3-phosphocholine bilayers by molecular dynamics simulations with the all-atom Optimised Potentials for Liquid Simulations and the coarse-grained MARTINI force field. On the statistically relevant time scales, the centre-of-mass mean-square displacement exhibits in both cases the subdiffusive asymptotic form $W(t) \sim 2D_\alpha t^\alpha$, with $\alpha \approx 0.67$ and $\alpha \approx 0.57$, respectively. The diffusive dynamics obtained by the MARTINI force field is, however, faster by a factor of about 3. The subdiffusive characteristics of the diffusion process is confirmed by comparing the integral of the centre-of-mass velocity autocorrelation function with its analytical long-time tail. The agreement is particularly good for the MARTINI force field, which permits to extend the simulation length and the system size considerably. Our results are in agreement with experimental observations of subdiffusion in lipid bilayers on longer time scales and do not support the finding of some authors that the latter should be considered as a transient phenomenon.

Keywords: anomalous diffusion; lipid bilayers; molecular dynamics simulations; coarse-grained force fields

1. Introduction

One of the most important molecular assemblies in living systems is the cell membrane, which consists of a lipid bilayer and embedded molecules. It delimits and protects the interior of the cell and permits communication with the exterior through a controlled bidirectional flow of energy and matter. In the liquid phase, biological membranes can be considered as two-dimensional fluids in which embedded molecules can diffuse arbitrarily far in the lateral dimensions. The advent of fluorescence-based techniques, such as fluorescence correlation spectroscopy (FCS) and single particle tracking (SPT) methods, revealed that the corresponding diffusion process is anomalous in the sense that the ensemble-averaged time-dependent mean square displacement (MSD)

$$W(t) = \langle (\mathbf{x}(t) - \mathbf{x}(0))^2 \rangle, \tag{1}$$

deviates from the linear form [1] found for the diffusion of molecules in normal liquids. One finds instead a sub-linear growth,

$$W(t) \overset{t\to\infty}{\sim} 2D_\alpha t^\alpha, \quad 0 < \alpha < 1, \tag{2}$$

where D_α is a fractional diffusion constant.[2–8] This type of anomalous diffusion is usually referred to as subdiffusion.[9] It is a characteristic property of 'crowded systems' in general and has also been observed in recent molecular dynamics (MD) computer simulations of lipid bilayers. [10–13] Subdiffusion can be understood by using the intuitive picture of the cage of instantaneous nearest neighbours, which captures the diffusing particle for a certain time. It depends now on the persistence time of this cage if normal diffusion or subdiffusion is observed. This aspect is developed in Ref. [14], establishing a relation to the classical theory of simple liquids.[15,16] The coefficient α indicates effectively how strongly the mean persistence time diverges and it should be considered as a mathematical quantity. A possible explanation of lateral subdiffusion in lipid bilayers is the strong entanglement of the lipid molecules, which hinders their motion considerably. We mention in this context that some authors consider subdiffusion as a transient phenomenon,[10,13] and even its existence is still under debate.[17] It is obvious that computer simulations cannot give a final clue to whether or not subdiffusion in lipid bilayers and biological membranes in general is only a transient phenomenon. The time scales accessible by MD simulation are still much shorter than those probed by FCS and SPT methods and the system size is very small. Simulations can, however, help to confirm or refute a diffusion model by looking at different statistical quantities, which are not necessarily accessible by experiments.

In order to extend the time scale and the system size accessible by MD simulations as much as possible, the use of coarse-grained (CG) simulation models is an interesting route to explore. By grouping several atoms into 'beads', the number of force centres and thus the computational

*Corresponding author. Email: gerald.kneller@cnrs-orleans.fr

effort of the force evaluation can be considerably reduced. We mention in this context Ref. [13], in which the MARTINI force field [18,19] is used to study lateral diffusion for different proteins in a lipid 1-palmitoyl-2-oleoyl-sn-glycero-3-phosphoethanolamine (POPE) / 1-palmitoyl-2-oleoyl-sn-glycero-3-phosphoglycerol (POPG) bilayer. Reducing the number of force centres leads, however, also inevitably to less friction and entanglement between the lipid molecules, such that their diffusion is enhanced.[19] The interesting question is, however, whether a detailed analysis of the lipid dynamics simulated with CG models approves or refutes the picture of anomalous lateral diffusion. This route is taken in this work, in which we study the lateral diffusion of lipid molecules in fully hydrated POPC (1-palmitoyl-2-oleoyl-sn-glycero-3-phosphocholine) bilayers, comparing the results obtained from MD simulations with the all-atom (AA) Optimised Potentials for Liquid Simulations (OPLS) force field [20,21] and the CG MARTINI force field. [18,19] To gain deeper insight into the diffusion process of the lipid molecules, we study in particular the relationship between the long-time behaviour of the velocity autocorrelation function (VACF) for the centre-of-mass of the lipids and the corresponding MSD.

2. Theoretical background

The asymptotic form of the MSD and the VACF can be related by means of asymptotic analysis, and their comparison yields deeper insight into the diffusion process under consideration.[14] This approach has been used in a recent study of lateral diffusion of lipid molecules in a DOPC (dioleoyl-sn-glycero-3-phosphocholine) membrane.[11] We found that the same method cannot be used for the POPC bilayers studied in this work, since the onset of the VACF long time tails falls in a time region in which the VACF data are already quite noisy. For this reason we consider here the time integral of the VACF, in which the statistical noise is to some extent removed by the integration procedure. The long-time behaviour of this integral has been discussed in Ref. [14] and we give here a short summary. We start with the MSD whose asymptotic form is supposed to be given by Equation (2). Asymptotic analysis [22] tells us then that its Laplace transform, which is defined through $\hat{W}(s) = \int_0^\infty \mathrm{d}t \exp(-st) W(t)$ ($\Re\{s\} > 0$) behaves for small s as

$$\hat{W}(s) \overset{s\to 0}{\sim} 2D_\alpha \Gamma(\alpha+1) s^{-(\alpha+1)}. \tag{3}$$

It follows on the other hand from $\mathbf{x}(t) = \int_0^t \mathrm{d}\tau \mathbf{v}(\tau)$ that [15]

$$W(t) = 2\int_0^t \mathrm{d}\tau (t-\tau) c_{vv}(\tau) \Leftrightarrow \hat{W}(s) = \frac{2\hat{c}_{vv}(s)}{s^2}, \tag{4}$$

where

$$c_{vv}(t) = \langle \mathbf{v}(t) \cdot \mathbf{v}(0) \rangle \tag{5}$$

is the VACF and $\hat{c}_{vv}(s)$ is its Laplace transform. Equating (3) and (4) one obtains

$$\frac{\hat{c}_{vv}(s)}{s} \overset{s\to 0}{\sim} D_\alpha \Gamma(\alpha+1) s^{-\alpha}. \tag{6}$$

Noting that $\hat{c}_{vv}(s)/s$ is the Laplace transform of

$$f_c(t) = \int_0^t \mathrm{d}\tau c_{vv}(\tau) \tag{7}$$

and that $0 < \alpha \leq 1$, it follows from a theorem in asymptotic analysis [22] that $f_c(t)$ has the asymptotic form

$$f_c(t) \overset{t\to\infty}{\longrightarrow} \alpha D_\alpha t^{\alpha-1}. \tag{8}$$

One recognises that the well-known Kubo formula for the normal diffusion coefficient, $D = \int_0^\infty \mathrm{d}\tau c_{vv}(\tau)$, is retrieved for $\alpha = 1$. The generalisation for this formula for anomalous diffusion follows from (6), employing the concept of fractional derivatives.[23] One obtains the generalised Kubo relation [14]

$$D_\alpha = \frac{1}{\Gamma(1+\alpha)} \int_0^\infty \mathrm{d}t \; {}_0\partial_t^{\alpha-1} c_{vv}(t), \tag{9}$$

where ${}_0\partial_t^{\alpha-1} c_{vv}(t)$ denotes a fractional Riemann–Liouville derivative of order $\alpha - 1$,

$${}_0\partial_t^{\alpha-1} c_{vv}(t) = \partial_t \int_0^t \mathrm{d}t' \frac{(t-t')^{\alpha-1}}{\Gamma(\alpha)} c_{vv}(t'). \tag{10}$$

To compare the diffusional behaviour of different systems, it is more convenient to work with the normalised VACF than with the VACF itself,

$$\psi(t) = \frac{c_{vv}(t)}{c_{vv}(0)}, \tag{11}$$

and the corresponding time integral fulfills the relation

$$f_\psi(t) = \int_0^t \mathrm{d}\tau \psi(\tau) \overset{t\to\infty}{\longrightarrow} \frac{\alpha D_\alpha}{\langle \mathbf{v}^2 \rangle} t^{\alpha-1}, \tag{12}$$

noting that $c_{vv}(0) = \langle \mathbf{v}^2 \rangle$.

3. MD simulation and analysis

For this comparative simulation study we constructed the following systems:

(1) A bilayer of 274 POPC lipids immersed in 10,471 water molecules for an MD simulation with a modified version of the AA OPLS force field. [20,21,24]
(2) A bilayer of 2033 CG POPC molecules immersed

in 231,808 water molecules for an MD simulation with the MARTINI force field.[18,19] The starting structure was taken from Ref. [25].

The simulated systems are shown in Figure 1. All MD simulations have been carried out with the GROMACS package,[26] using version 4.5.4 for the OPLS and version 4.6.1 for the MARTINI force field. In all cases, periodic boundary conditions were applied and chemical bonds involving hydrogen atoms were constrained to constant lengths using the linear constraint solver algorithm.[27] Depending on the system, specific choices were made for the thermodynamic ensemble and other control parameters of the MD algorithm:

(1) *AA model*: After an equilibration phase of 230 ns we carried out a production run of 15 ns in the NpT-ensemble, using the Nosé–Hoover extended system method [28,29] with an anisotropic Parrinello–Rahman barostat [30] and an integration step of 1 fs. Electrostatic interactions were treated with the particle-mesh Ewald method,[31] using a real space cut-off of 1.2 nm. The same cut-off was taken for the van der Waals interactions.
(2) *CG model*: after an equilibration phase of 1200 ns, the simulation of the CG model was carried out for 600 ns, using a time step of 30 fs. Electrostatic and van der Waals interactions were smoothly switched to zero in a defined distance range, $r_{\min} \le r \le r_{\max}$ (see Ref. [19] and references herein). For our simulations we used $r_{\min} = 0.9$ nm and $r_{\min} = 0$ nm for van der Waals and Coulomb interactions, respectively, and $r_{\max} = 1.2$ nm for both van der Waals and Coulomb interactions.

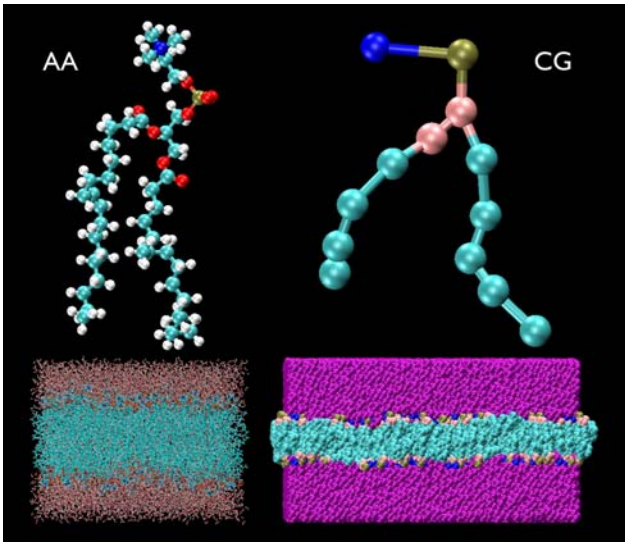

Figure 1. Simulated POPC bilayers using an OPLS AA force field (left) and a CG MARTINI force field (right). The upper part of the figure shows the representation of the lipid molecules.

An important point to be observed in the context of this study is that the masses of the lipid molecules in the MARTINI force field are increased from the physical value of $M = 760.08$ amu to $M_{CG} = 936$ amu ('amu' stands for atomic mass units). This slows the molecular motions down and leads in particular to a reduction of the fractional diffusion constant. Equation (9) shows that the latter is proportional to the VACF, and since $c(0) = \langle \mathbf{v}^2 \rangle = 2k_B T/M$ the increased mass leads to a reduction of D_α by a factor of $M/M_{CG} \approx 0.8$. To accelerate the diffusional motion, we simulated the system at slightly higher temperature of 320 K. The temperature raise from 310 K to 320 K leads to an estimated increase of the diffusion coefficient by a factor of about by 25% [32] and thus to a compensation of the mass effect. Two different thermodynamic conditions were considered for the simulations.

(a) Simulation at constant surface in the lateral dimensions of the bilayer, maintaining the temperature at $T = 320$ K and the pressure perpendicular to the bilayer at 1 atm ('NAp$_z$T-ensemble'). The method is described in Ref. [19]
(b) Simulation at constant volume, maintaining the temperature at $T = 320$ K with the Berendsen thermostat.[33]

From the centre-of-mass trajectories of the lipid molecules we computed the corresponding MSDs and VACFs according to

$$W_j(n) \approx \frac{1}{N_t - n} \sum_{k=0}^{N_t - n - 1} \left(\mathbf{x}_j(k+n) - \mathbf{x}_j(k)\right)^2, \qquad (13)$$

$$c_j(n) \approx \frac{1}{N_t - n} \sum_{k=0}^{N_t - n - 1} \mathbf{v}_j(k) \cdot \mathbf{v}_j(k+n), \qquad (14)$$

where N_t is the number of time steps in the MD trajectory and $\mathbf{x}(n) \equiv \mathbf{x}(n\Delta t)$, where Δt is the sampling time step. Both MSD and VACF have been computed using a 'detour' via Fast-Fourier transform to speed up the calculations.[34–36] In order to improve the statistical accuracy of our calculations, we averaged the molecular quantities over all N (physically equivalent) molecules,

$$W(n) = \frac{1}{N} \sum_{k=1}^{N} W_j(n), \qquad (15)$$

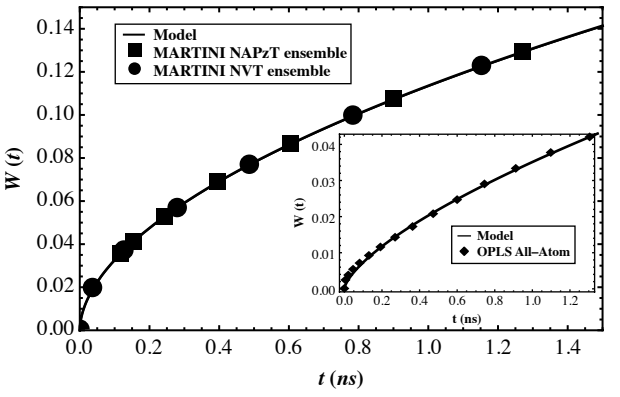

Figure 2. MSDs for the lateral centre-of-mass diffusion of POPC molecules simulated with the OPLS AA force field in the NpT ensemble (diamonds) and with the MARTINI force field, using the NVT and the NAp_zT ensemble (circles and squares, respectively).

$$c(n) = \frac{1}{N}\sum_{k=1}^{N} c_j(n). \tag{16}$$

The integral of the normalised VACF was computed according to the central difference scheme

$$f_\psi(n) \approx \sum_{k=0}^{n} \frac{\Delta t}{12}\big(8\psi(k) + 5\psi(k-1) - \psi(k+1)\big), \tag{17}$$

where Δt is again the sampling step and $0 < n < N_t - 1$.

4. Results

Figure 2 shows a comparison of the lateral MSDs of the POPC molecules obtained from the OPLS and the CG MARTINI force field, respectively. The lag time scale of 1.5 ns corresponds to 10% of the total simulation length with the OPLS. We found in many simulations of different systems that the maximum MSD lag time should not exceed about 10% of the total simulation length if the MSD can be averaged over several 100 or (better) 1000 physically equivalent particles. In case of single molecule MSDs, the accessible lag time is even much shorter. Both simulation potentials clearly lead to subdiffusive MSDs, in which the diffusion obtained with the MARTINI force field is about three times faster. On the lag time scale of 1.5 ns, the NAp_zT and the NVT ensembles used with the MARTINI force field lead to almost identical curves. The values for α and D_α, which are given in Table 1, have been obtained by fitting expression (2) for the full time interval of $0 \le t \le 1.5$ ns. One observes that the α-coefficient for the simulation with the OPLS force field is slightly higher than the one obtained with the MARTINI force field, indicating that the diffusional motion is slightly more 'normal' than in the latter case. The diffusion coefficient for the OPLS force field may be compared with that obtained for the DOPC bilayer studied with the same force field in Ref. [11]. The value found for DOPC on a 30 ns lag time scale was $0.101\,\mathrm{nm}^2/\mathrm{ns}^\alpha$, with $\alpha = 0.61$. Compared with the POPC simulation presented here, the diffusional characteristics is thus the same, but the diffusion is twice faster. The reason is that DOPC is more fluid than POPC, its transition to the liquid phase occurring already at a temperature of 256 K instead at 270 K for POPC.[37,38] The experimental value for lateral diffusion in specific biological cell membranes found in [3], $D_\alpha \approx 0.088\,\mathrm{nm}^2/\mathrm{ns}^\alpha$ with $\alpha \approx 0.74$ (the units have been converted here), is compatible with the results of the MD simulations of DOPC and POPC bilayers with the OPLS force field described above. We mention here that biological membranes contain mixtures of different lipid molecules. Figure 3 displays the lateral MSDs for the MARTINI force field for the whole accessible lag time scale, which is about 40 times longer than for the MD simulation with the OPLS force field. Table 1 shows that D_α and α stay very close to the values obtained for the shorter 1.5 ns time scale, preserving even the relationships between the results for the NAp_zT and NVT simulations. We note here that the value for the fractional diffusion coefficient corresponding to the OPLS force field stays quite stable if the production run and the corresponding maximum lag time are extended to 150 and 15 ns, respectively. In this case we find $D_\alpha = 0.016\,\mathrm{nm}^2/\mathrm{ns}^\alpha$ with $\alpha \approx 0.701$.

Figures 4–6 show the normalised VACFs together with their integrals (insets) for the OPLS and the two simulations with the MARTINI force field, respectively. There is a clear difference between the VACFs for the OPLS and the MARTINI force field. One recognises that the minimum of the VACF in the latter case is less

Table 1. Coefficient α and fractional diffusion coefficient D_α for the OPLS AA simulation of POPC and the CG MARTINI force field.

	AA 1.5 ns	CG (1) 1.5 ns	CG (2) 1.5 ns	CG (1) 50 ns	CG (2) 50 ns
α	0.668	0.515	0.508	0.571	0.558
D_α [nm^2/ns]	0.018	0.057	0.058	0.051	0.051

Note: Here (1) and (2) refer, respectively, to the simulation with the NAp_zT and NVT ensembles described in the text.

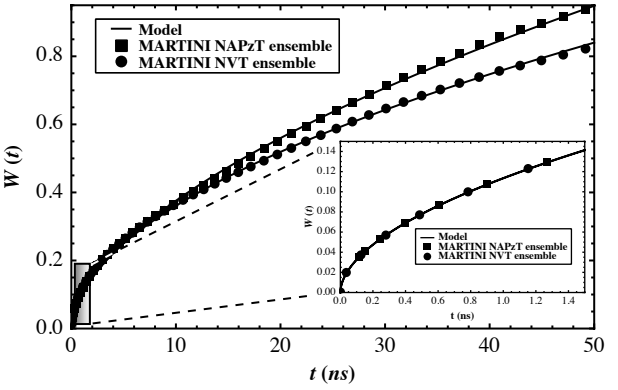

Figure 3. MSDs for the lateral centre-of-mass diffusion of POPC molecules simulated with the MARTINI force field in the NVT and NAp_zT ensemble on a longer lag time scale (circles and squares, respectively). The inset shows the corresponding quantities on the same scale as in Figure 2.

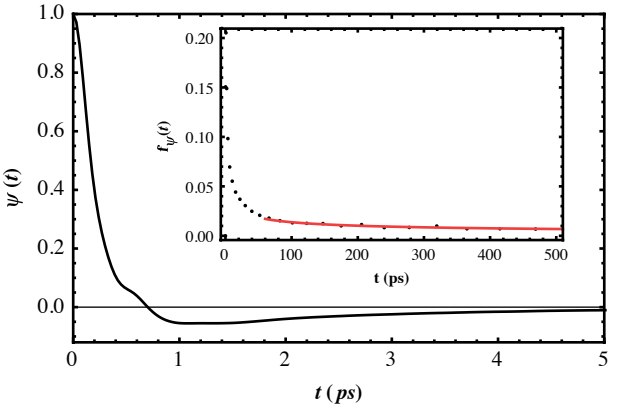

Figure 5. (Color online) Normalised VACFs for the lateral centre-of-mass motion of POPC molecules simulated with the MARTINI force field in the NAp_zT ensemble. The inset shows the numerical integral (dots) and the analytical long-time tail $f_\psi(t)$ (red solid line).

pronounced than in the first case, indicating a smaller cage effect for short times. This is consistent with the observation that the lateral diffusion obtained with the MARTINI force field is faster. One observes also a difference in the form of the VACFs for small times, which is due to the fact that the forces determining the 'rattling' motions in the cage of nearest neighbours are not the same. This point is, however, not important in the context of this study, since only the *asymptotic* form of the VACF is relevant for the diffusional characteristics of the lipid molecules. The VACFs obtained for the two different thermodynamic ensembles (NAp_zT and NVT) with the MARTINI force field are, in contrast, indistinguishable on the time scale of 5 ps. This finding is in agreement with the observation that the corresponding MSDs for short times are identical (Figure 2). Comparing the analytical and numerical values for the long time tails of the integrated VACFs, which are shown in the insets of Figures 4–6, respectively, clearly confirms the observation of subdiffusion. Here one observes that the agreement is much better for the MARTINI force field, which can be attributed to the considerable increase of the statistical accuracy for this type of simulation. Not only the available MD trajectories are 40 times longer than for the OPLS, but also the number of physically equivalent lipid molecules, N, appearing in expressions (13) and (14) is more than seven times larger.

5. Conclusion

Our findings clearly support the experimental observations of lateral subdiffusion in biological membranes, in which the OPLS force field and the MARTINI force field lead to similar α-coefficients but different fractional diffusion constants. The diffusion found for the OPLS force field is of the right order of magnitude compared with

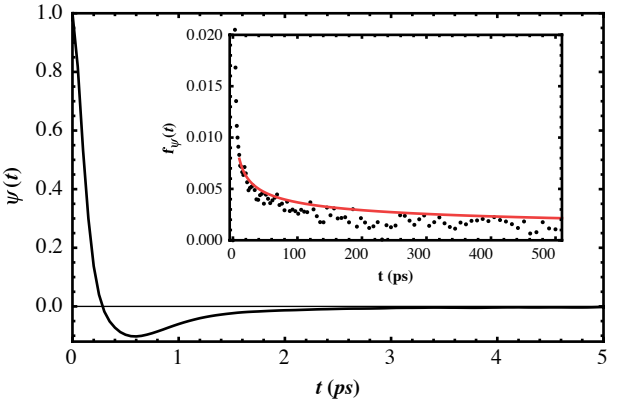

Figure 4. (Color online) Normalised VACFs for the lateral centre-of-mass motion of POPC molecules simulated with the OPLS force field in the *NPT* ensemble. The inset shows the numerical integral (dots) and the analytical long-time tail $f_\psi(t)$ (red solid line).

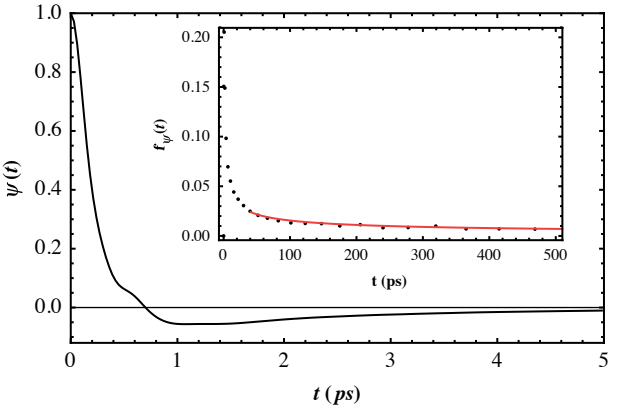

Figure 6. (Color online) Normalised VACFs for the lateral centre-of-mass motion of POPC molecules simulated with the MARTINI force field in the NVT ensemble. The inset shows the numerical integral (dots) and the analytical long-time tail $f_\psi(t)$ (red solid line).

experimental studies with FCS on cell membranes, but seems to be overestimated by the MARTINI force field. The asymptotic form of the VACF integrals confirms the subdiffusion seen in the MSDs by independent numerical calculations and demonstrates the importance of statistical accuracy for a meaningful analysis of the diffusional motion in complex molecular systems. Here the CG MARTINI force field provides an important mean to the study of transport processes in membranes since it permits to extend the length and time scales of the simulated systems considerably. It would be worth trying to reduce the overestimation of the fractional diffusion constant by tuning the force field parameters correspondingly.

Acknowledgement

Sławomir Stachura acknowledges financial support by the Agence Nationale de la Recherche (Contract No. ANR-2010-COSI-001-01).

References

[1] Einstein A. Über die von der molekularkinetischen Theorie der Wärme geforderte Bewegung von in ruhenden Flüssigkeiten suspendierten Teilchen. Ann Phys. 1905;322(8):549–560.
[2] Schwille P, Haupts U, Maiti S, Webb W. Molecular dynamics in living cells observed by fluorescence correlation spectroscopy with one-and two-photon excitation. Biophys J. 1999;77(4):2251–2265.
[3] Schwille P, Korlach J, Webb W. Fluorescence correlation spectroscopy with single-molecule sensitivity on cell and model membranes. Cytometry. 1999;36(3):176–182.
[4] Ratto TV, Longo ML. Anomalous subdiffusion in heterogeneous lipid bilayers. Langmuir. 2003;19(5):1788–1793.
[5] Ritchie K, Shan X-Y, Kondo J, Iwasawa K, Fujiwara T, Kusumi A. Detection of non-Brownian diffusion in the cell membrane in single molecule tracking. Biophys J. 2005;88(3):2266–2277.
[6] Dworecki K. Experimental investigation of the subdiffusion in a membrane system. Phys A Stat Mech Appl. 2006;359:24–32.
[7] Forstner MB, Martin DS, Rückerl F, Käs J, Selle C. Attractive membrane domains control lateral diffusion. Phys Rev E. 2008;77(5):051906 (7 pages).
[8] Weigel AV, Simon B, Tamkun MM, Krapf D. Ergodic and nonergodic processes coexist in the plasma membrane as observed by single-molecule tracking. Proc Natl Acad Sci. 2011;108(16):6438–6443.
[9] Metzler R, Klafter J. The random walk's guide to anomalous diffusion: a fractional dynamics approach. Phys Rep. 2000;339(1):1–77.
[10] Flenner E, Das J, Rheinstädter MC, Kosztin I. Subdiffusion and lateral diffusion coefficient of lipid atoms and molecules in phospholipid bilayers. Phys Rev E. 2009;79(1):11907 (11 pages).
[11] Kneller GR, Baczynski K, Pasenkiewicz-Gierula M. Communication: consistent picture of lateral subdiffusion in lipid bilayers: molecular dynamics simulation and exact results. J Chem Phys. 2011;135(14):141105 (4 pages).
[12] Jeon JH, Monne HMS, Javanainen M, Metzler R. Anomalous diffusion of phospholipids and cholesterols in a lipid bilayer and its origins. Phys Rev Lett. 109:188103 (4 pages).
[13] Goose JE, Sansom MSP. Reduced lateral mobility of lipids and proteins in crowded membranes. PLoS Comput Biol. 2013;9(4):e1003033 (10 pages).
[14] Kneller GR. Generalized Kubo relations and conditions for anomalous diffusion: physical insights from a mathematical theorem. J Chem Phys. 2011;134:224106 (7 pages).
[15] Boon JP, Yip S. Molecular hydrodynamics. New York, NY: McGraw Hill; 1980.
[16] Hansen J-P, McDonald IR. Theory of simple liquids. 2nd ed. Amsterdam: Academic Press; 1986.
[17] Saxton MJ. Wanted: a positive control for anomalous subdiffusion. Biophys J. 2012;103(12):2411–2422.
[18] Marrink SJ, de Vries AH, Mark AE. Coarse grained model for semiquantitative lipid simulations. J Phys Chem B. 2004;108(2):750–760.
[19] Marrink SJ, Jelger Risselada H, Yefimov S, Peter Tieleman D, de Vries AH. The MARTINI force field: coarse grained model for biomolecular simulations. J Phys Chem B. 2007;111(27):7812–7824.
[20] Jorgensen WL, Tirado-Rives J. The OPLS [optimized potentials for liquid simulations] potential functions for proteins, energy minimizations for crystals of cyclic peptides and crambin. J Am Chem Soc. 1988;110(6):1657–1666.
[21] Jorgensen WL, Maxwell DS, Tirado-Rives J. Development and testing of the OPLS all-atom force field on conformational energetics and properties of organic liquids. J Am Chem Soc. 1996;118(45):11225–11236.
[22] Karamata J. Neuer Beweis und Verallgemeinerung der Tauberschen Sätze, welche die Laplacesche und Stieltjessche Transformation betreffen. J Reine Angew Math. 1931;1931(164):27–39.
[23] Oldham KB, Spanier J. The fractional calculus. New York, London: Academic Press; 1974.
[24] Murzyn K, Rog T, Jezierski G, Takaoka Y, Pasenkiewicz-Gierula M. Effects of phospholipid unsaturation on the membrane/water interface: a molecular simulation study. Biophys J. 2001;81(1):170–183.
[25] Loeffler HH, Winn MD. Large biomolecular simulation on HPC platforms I. Experiences with AMBER, GROMACS and NAMD. Technical Report, UK Science & Technology Facilities Council, September 2009.
[26] Hess B, Kutzner C, van der Spoel D, Lindahl E. GROMACS 4: algorithms for highly efficient, load-balanced, and scalable molecular simulation. J Chem Theory Comput. 2008;4(3):435–447.
[27] Hess B, Bekker H, Berendsen HJC, Fraaije JGEM. LINCS: a linear constraint solver for molecular simulations. J Comput Chem. 1997;18(12):1463–1472.
[28] Nosé S. A unified formulation of the constant temperature molecular dynamics methods. J Chem Phys. 1984;81(1):511–519.
[29] Hoover WG. Canonical dynamics: equilibrium phase-space distributions. Phys Rev A. 1985;31(3):1695–1697.
[30] Parrinello M. Polymorphic transitions in single crystals: a new molecular dynamics method. J Appl Phys. 1981;52(12):7182–7190.
[31] Essmann U, Perera L, Berkowitz M, Darden T, Lee H, Pedersen LG. A smooth particle mesh Ewald method. J Chem Phys. 1995;103(19):8577–8593.
[32] Köchy T, Bayerl TM. Lateral diffusion coefficients of phospholipids in spherical bilayers on a solid support measured by ^{2}H resonance relaxation. Phys Rev E. 1993;47(3):2109–2116.
[33] Berendsen HJC, Postma JPM, van Gunsteren WF, DiNola A, Haak JR. Molecular dynamics with coupling to an external bath. J Chem Phys. 1984;81(8):3684–3690.
[34] Kneller GR, Keiner V, Kneller M, Schiller M. nMmoldyn – a program package for a neutron-scattering oriented analysis of molecular-dynamics simulations. Comput Phys Commun. 1995;91(1-3):191–214.
[35] Rog T, Murzyn K, Hinsen K, Kneller GR. nMoldyn: a program package for a neutron scattering oriented analysis of molecular dynamics simulations. J Comput Chem. 2003;24(5):657–667.
[36] Brigham EO. The fast Fourier transform. Englewood Cliffs, NJ: Prentice Hall; 1974.
[37] Lewis RN, Sykes BD, McElhaney RN. Thermotropic phase behavior of model membranes composed of phosphatidylcholines containing cis-monounsaturated acyl chain homologues of oleic acid: differential scanning calorimetric and 31P NMR spectroscopic studies. Biochemistry. 1988;27(3):880–887.
[38] Litman BJ, Lewis EN, Levin IW. Packing characteristics of highly unsaturated bilayer lipids: Raman spectroscopic studies of multilamellar phosphatidylcholine dispersions. Biochemistry. 1991;30(2):313–319.